SCIENCE CHINA
Information Sciences

• LETTER •

July 2026, Vol. 69, Iss. 7, 179401:1–179401:2
https://doi.org/10.1007/s11432-025-4582-7

Scattering-suppression induced two-dimensional hole gas mobility enhancement in GaN p-FETs with a multiperiod scattering-modulated barrier layer

Xu LIU, Shengrui XU*, Hongchang TAO*, Huake SU*, Tao ZHANG, Lei XIE, Xinhao WANG, Yuan GAO, Jincheng ZHANG & Yue HAO

State Key Laboratory of Wide-Bandgap Semiconductor Devices and Integrated Technology, School of Microelectronics, Xidian University, Xi'an 710071, China

Received 25 June 2025/Revised 3 August 2025/Accepted 7 September 2025/Published online 27 April 2026

Citation Liu X, Xu S R, Tao H C, et al. Scattering-suppression induced two-dimensional hole gas mobility enhancement in GaN p-FETs with a multiperiod scattering-modulated barrier layer. Sci China Inf Sci, 2026, 69(7): 179401, https://doi.org/10.1007/s11432-025-4582-7

GaN has emerged as a cornerstone material for high-power electronic devices and radio frequency applications [1]. The GaN-based p-type field-effect transistors (p-FETs) represent a significant impediment to the development of all-GaN complementary logic circuits. The primary cause of the substandard performance of p-FETs is low conductivity. The mobility of the two-dimensional hole gas (2DHG) typically remains below 15 $\mathrm{cm^2/(V\cdot s)}$, which is significantly lower than that of the two-dimensional electron gas (2DEG) [2]. Presently, there is an absence of effective methodologies to augment hole mobility, a critical factor for high-performance p-FETs.

The present study has yielded an enhanced-mobility GaN-based p-FET with a multiperiod scattering-modulated barrier (MSB) layer. The MSB layer contains six-period $Al_{0.15}Ga_{0.85}N$/GaN heterostructures. A comparative analysis was conducted between p-FETs utilizing MSB layers and p-FETs with AlGaN barrier layers. The former exhibited a 26.8% enhancement in hole mobility. The p-FETs with the MSB layer exhibited superior performance, indicating ample potential for future advancements in this field.

Experiment. Figure 1(a) illustrates the epi-layer grown on a sapphire substrate by metal organic chemical vapor deposition. This process incorporates a 2 μm-thick GaN buffer layer, an MSB layer comprising six periods 20 nm $Al_{0.15}Ga_{0.85}N$/6 nm GaN, a 1.5 nm-thick AlN insertion layer, a 10 nm-thick unintentionally doped GaN (u-GaN), and a 30 nm-thick p-GaN ([Mg]: $3\times10^{19}\ \mathrm{cm^{-3}}$). As shown in Figure 1(b), the conventional p-FET with a 33 nm $Al_{0.25}Ga_{0.75}N$ barrier layer is utilized for comparison. The samples with the MSB layer and the AlGaN barrier layer are designated as Samples A and B, respectively.

The fabrication process of the devices began with mesa isolation by ICP etching, resulting in a total depth of approximately 250 nm. Subsequently, a Ni/Au (30/100 μm) metal stack was deposited on the source and drain regions and annealed in an O_2 atmosphere. A low-damage ICP was employed to pattern the gate region, with a total etch depth of 15 nm. The fabrication of the gate electrodes entailed the deposition of a W/Au (30/150 nm) metal stack on the gate region. The fabricated p-FETs have gate, source-gate, and source-drain lengths of 2, 2, and 6 μm, respectively.

Results and discussion. The effect of AlGaN and GaN layer thicknesses in the MSB layer on hole concentration was investigated using TCAD. The optimized MSB layer consists of 6-period 20 nm $Al_{0.15}Ga_{0.85}N$/6 nm GaN structures. The band structures and hole distributions of the two samples are shown in Figures 1(c) and (d). As demonstrated in Sample A, there is a higher peak hole concentration in comparison to Sample B. This finding suggests that the MSB layer enables a higher hole concentration with a lower Al composition. The Hall Effect measurements indicated that the sheet hole density (SHD) and mobility of Sample A were $8.28\times10^{12}\ \mathrm{cm^{-2}}$ and 17.5 $\mathrm{cm^2/(V\cdot s)}$, respectively. The SHD and mobility of Sample B were $8.13\times10^{12}\ \mathrm{cm^{-2}}$ and 13.8 $\mathrm{cm^2/(V\cdot s)}$, respectively. Sample A exhibited an increase in SHD and mobility in comparison to Sample B. Additionally, the material properties of both samples were characterized. As shown in Figures 1(e) and (f), the surface morphology is characterized by atomic force microscopy. Samples A and B demonstrate step-flow morphology and comparable root mean square roughness, indicating similar interfacial properties. As shown in Figures 1(g) and (h), the crystal quality of the two samples is examined using high-resolution X-ray diffraction. The increase in threading dislocation density in Sample A, as compared to Sample B, is attributed to the growth of a multiperiod heterojunction. Despite the elevated dislocation density in Sample A, it nevertheless exhibits a higher SHD. As shown in Figure 1(i), the strain state of the two samples is characterized using Raman measurements. The E_2 (high) peaks of GaN for Samples A and B are 570.8 and 570.2 $\mathrm{cm^{-1}}$, respectively. Higher biaxial compressive strain, as observed in Sample A, results in higher piezoelectric polarization in GaN compared to Sample B. The enhanced piezoelectric polarization increases the negative polarization charges at the 2DHG channel of Sample A, thereby attracting more holes to accumulate. This is the primary reason why Sample A has a higher SHD. In addition to the enhanced SHD, Sample A demonstrates a 26.8% higher mobility in

* Corresponding author (email: srxu@xidian.edu.cn, taohongchang@xidian.edu.cn, huakexidian@126.com)

© Science China Press 2026

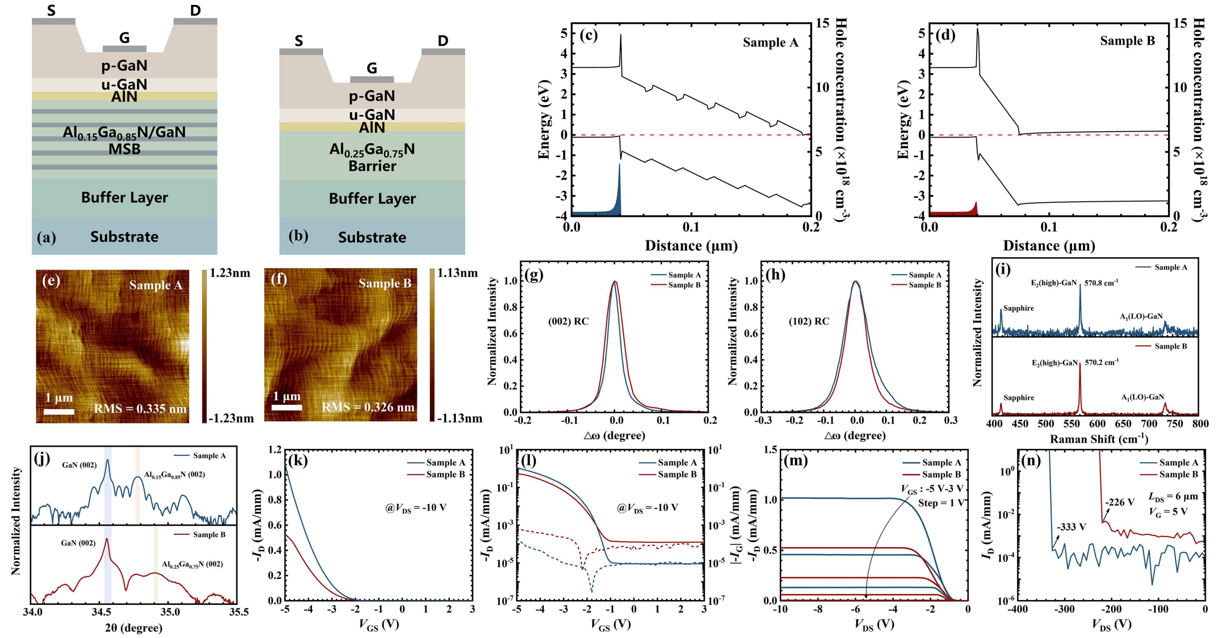

Figure 1 (Color online) Schematic of the p-FETs with (a) MSB layers and (b) conventional AlGaN barrier layers. Band structures and hole distributions of (c) Sample A and (d) Sample B. 5 × 5 μm^2 atomic force microscope images of (e) Sample A and (f) Sample B. (g) (002), (h) (102) plane XRCs, (i) Raman spectra and (j) (0002) plane 2θ curves of Samples A and B. Transfer characteristics plotted in (k) linear and (l) logarithmic scales. (m) Output characteristics and (n) breakdown characteristics of Samples A and B.

comparison to Sample B.

The hole mobility is predominantly influenced by the hole effective mass and scattering effects. For the two samples under biaxial compressive strain, the hole effective mass is found to be identical. The observed variations in hole mobility are predominantly attributable to disparities in the scattering effects. At 300 K, the following scattering mechanisms predominate, with their respective impacts on mobility listed in descending order: polar optical phonon (POP) scattering, alloy disorder scattering (ADO), interface roughness scattering (IFR), and acoustic deformation potential scattering (ADP). Given the similarity of the materials utilized in both samples and the uniformity of the testing environments and comparable carrier concentrations, the POP and ADP scattering exhibit analogous intensities. As illustrated in Figure 1(j), the (0002) plane 2θ curves of the samples are presented. The position of the AlGaN peak is 34.77° and 34.91° for Samples A and B, respectively. The calculated Al compositions for Samples A and B are 15% and 25%, respectively. The reduced Al composition serves to mitigate local potential fluctuations caused by chemical and positional disorder, thereby enhancing the translational symmetry of the crystal lattice. Consequently, ADO scattering in Sample A demonstrates a decrease compared to Sample B, which is the primary factor contributing to the enhancement in the mobility of Sample A. The long-range Coulombic scattering from the 2DEG channel exerts a considerable influence on the hole mobility. The MSB layer (150 nm) demonstrates increased thickness relative to the conventional barrier layer (33 nm). The two channels in Sample A demonstrate enhanced spatial separation, thereby suppressing the Coulombic interaction and enhancing mobility.

To investigate the effect of the MSB layer on device performance, the p-FETs based on Samples A and B were fabricated. The transfer characteristics of the devices are depicted in Figures 1(k) and (l), respectively, in both linear and logarithmic scales. Samples A and B demonstrate enhancement-mode operation, exhibiting a comparable threshold voltage of −2 V. Sample A exhibits a higher $I_{\rm D}$ attributed to its enhanced conductivity. The output characteristics of the devices are illustrated in Figure 1(m), and the breakdown voltage of the devices is presented in Figure 1(n). Sample A achieved a saturation current density of 1.02 mA/mm at a $V_{\rm GS}$ of −5 V, demonstrating a 94.3% enhancement compared to Sample B. Although Sample A exhibits a higher dislocation density compared to Sample B, it also demonstrates superior breakdown voltage. The MSB layer in Sample A enhances reverse blocking capability in GaN p-FETs by constructing a thicker back barrier layer. In addition, multiperiod heterostructures are characterized by the presence of numerous high-energy barriers. These barriers confine holes through band bending and suppress vertical leakage. Consequently, the device equipped with an MSB layer attains a −333 V breakdown voltage (1.66 MV/cm), marking a 47% increase compared to conventional devices.

Conclusion. In conclusion, this work demonstrates that the p-FET with the MSB layer achieves higher performance than the conventional p-FET. The p-FET with an MSB layer demonstrates superior SHD and a 26.8% enhancement in hole mobility. A higher saturation current is observed for the p-FET with the MSB layer. The saturation current has been augmented by 94.3%. The p-FET with the MSB layer exhibits a higher breakdown voltage. The implementation of the MSB layers offers a novel methodology for the design of GaN-based p-FETs and complementary logic circuits.

Acknowledgements This work was supported by National Key R&D Program of China (Grant No. 2022YFB3604400), Natural Science Basic Research Program of Shaanxi (Grant No. 2023-JC-JQ-56), National Natural Science Foundation of China (Grant Nos. 62074120, 62404167, and 62134006), Postdoctoral Fellowship Program of China Postdoctoral Science Foundation (Grant No. GZC20241306), and Fundamental Research Funds for the Central Universities (Grant Nos. ZYTS25216, ZYTS25225).

References

1 Bader S, Lee H, Chaudhuri R, et al. Prospects for wide bandgap and ultrawide bandgap CMOS devices. IEEE Trans Electron Devices, 2020 67: 4010–4020
2 Liu X, Xu S, Zhang T, et al. Demonstration of a GaN-based P-channel FinFET with high current density based on multi-channel structure. Appl Phys Lett, 2025 126: 202103